LA-UR- 00-5335

Approved for public release; distribution is unlimited.

Title: HIGH SPEED OPTICAL AND X-RAY METHODS FOR EVALUATING LASER-GENERATED SHOCK-WAVES IN MATERIALS

Author(s): Dennis L. Paisley, Damian C. Swift, Andrew C. Forsman, George A. Kyrala, Raldall P. Johnson, all P-24
Roger A. Kopp, X-1
Justin C. Wark, Oxford University, Oxford, England
Adrian Allen , Oxford University, Oxford, England
Andrew Loveridge, Oxford University, Oxford, England

Submitted to: Proceedings of the 24th International Congress on High Speed Photography and Photonics, Sept. 24-29,2000, Sendai, Japan, to be published by the SPIE- the International Society for Optical Engineering

Los Alamos
NATIONAL LABORATORY

DISCLAIMER

High-speed optical and x-ray methods for evaluating laser-generated shock-waves in materials, and the corresponding dynamic material response

D. L. Paisley*[a], D. C. Swift[a], A. C. Forsman[a], G. A. Kyrala[a], R. P. Johnson[a], J. S.Wark[b], A. Allen[b], A. Loveridge,[b] R. A. Kopp[a]

[a] Los Alamos National Laboratory, Los Alamos, NM 87545
[b] Oxford University, Oxford, UK

e-mail: paisley@lanl.gov

1. X-ray, diffraction, VISAR, interferometry, streak photography, x-ray streak photography, silicon, beryllium

ABSTRACT

Optical diagnostic techniques including interferometry, electronic streak photography, and transient x-ray diffraction are used to study the dynamic material response to shock loading by direct laser irradiation and impact by laser-launched plates. The Los Alamos Trident laser is one of several lasers that have been used to generate shocks of 10 Kbar to several Mbar in single crystal and polycrystalline materials. Incorporating optical velocity interferometry (line-VISAR and point-VISAR) with transient x-ray diffraction can provide a complete understanding of the dynamic material response to shock compression and release.

Laser-launched flyer plates provide an ideal method to generate one-dimensional shocks in materials. The quality of the one-dimensionality of the launch and acceleration of plates is evaluated by line-imaging VISAR. The line-imaging VISAR images the fringes along a line across the diameter of the plate. Each fringe maxima and minima provide acceleration and velocity information at the specific point on the plate. By varying the fringe constant, number of fringes and fringe spacing on the plate, detailed experimental data can be obtained. For our experiments, most plates are 3-mm diameter and accelerated to 0.2 — >6 km/sec.

1. Introduction

Lasers provide an ideal experimental method to study the dynamics of materials under shock compression and release by direct laser shock and laser-launched flyer plates. Large laboratory lasers that can vary pulse length over one or two orders of magnitude can launch plates or provide direct well-controlled shocks from a few 10 s kilobars to several megabars. Optical and x-ray high-speed diagnostics can be easily synchronized with the laser and associated electronic diagnostics. The Los Alamos Trident laser has been used to generate laser-shocks by direct drive, indirect drive (hohlraums) and launch flyer plates for impact on target test samples. By properly designing an experiment with laser parameters shock durations <100-ps to > 200-ns can be produced in traditional and non-traditional materials on a mesoscale to microscale (pseudo-bulk to sub-grain size, and single crystal). Laser-launched flyer plates broaden the experimental methods for studying hydrodynamics of materials, and provides new capabilities to experimentally validate material models over a large range of pressure and pulse duration. The laser-launched flyer plates provides and intermediate capability between direct laser shocks and gas-gun launched flyer plates for shocks. In general, direct laser shocks are difficult at low pressures (10-100 kbar) at long durations (100 ns), and gas guns shocks are difficult at high pressures (>1 Mbar) and short duration (<1 — 100 ns). Laser-launched plates can adequately generate 10 kbar —≥ 1 Mbar at varying pulse duration from <1 - ≥ 10 ns, and can easily be synchronized to laboratory experimental equipment.

This work was performed under the auspices of the U.S. Department of Energy, DOE Contract No. W-7405-ENG-36.

2.Trident laser

1.1. Laser parameters

The Trident laser driver consists of a Nd:YLF master oscillator with a chain of Nd:phosphate glass amplifiers as a conventional master-oscillator, power amplifier (MOPA). The laser has three separate beams with an energy output of 250 Joules at 2ω (527 nm) from each of two beams, and a third beam at 50 Joules. The pulse shape and duration can be varied from less than 100 picoseconds to greater than several 100 s of nanoseconds. The oscillator output pulse is temporally shaped, and amplified. Either of the 250 Joule beams may be used to provide an x-ray source for transient x-ray diffraction (time-resolved Bragg and Laue), and the other for shock generation in the target. For x-ray diffraction, the laser is normally operated at 527 nm (2 ω), and for launching flyer plates the fundamental mode, 1054-nm is used. The third beam can be timed to occur before or after the main drive beams and used as an optical probe, x-ray backlighting, launching flyer plates or target diagnostics. Beams can be focused on a target in a vacuum containment chamber incorporating various optical, x-ray and electronic ports for diagnostics.

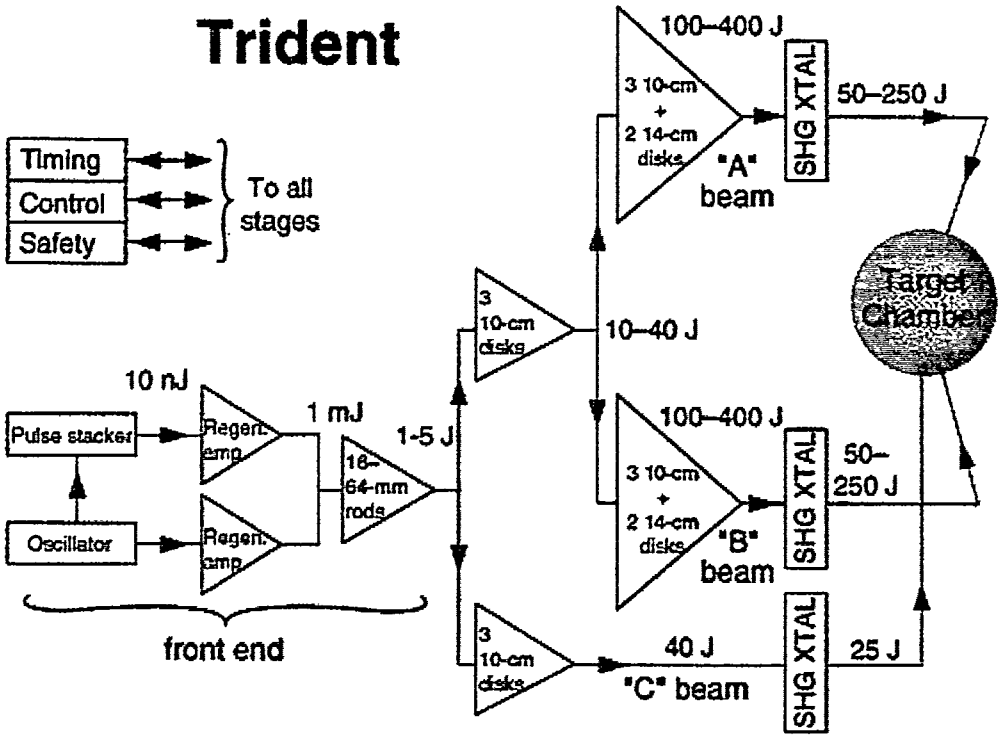

Figure 1: The Trident laser has three beams (250 J, 250 J, 50 J) that can be used for direct shocks, indirect shocks, or laser-launched flyer plates.

3.Optical and x-ray high speed diagnostics methods

The laser pulse profile is shaped both spatially and temporally to provide the proper direct drive for shocked single crystal and for laser-launched flyer plates. Laser spatial and temporal profiles are recorded with CCD cameras and photodiodes, respectively. The diagnostic methods to record the dynamic response of materials include: point-VISAR, line-imaging VISAR, and transient x-ray diffraction. The temporal resolution of all three diagnostics is <100-ps.

3.1. Dynamic x-ray diffraction of shocked single crystals

X-rays can probe single crystal solids and provide insight as to their atomic-level structure. The dynamics and time dependence of these structures under shock loading and release is important in understanding elastic and elastic-plastic response, and how materials transform and/or recover. Understanding dynamic material response on the single crystal or grain level can provide a basis of understanding and modeling bulk polycrystalline materials.[1-5]

4.Dynamic x-ray diffraction of shocked single crystals

4.1. x-ray diffraction experimental method

A uniaxial shock is generated in a single crystal by either direct laser irradiation. While the shock is propagating through the crystal a second laser beam focused to ~100- m spot at 10^{13-15} W/cm^2 to excite aline radiation of the x-source. With the point source line x-ray placed near the static Bragg angle for the crystal, an x-ray streak camera and time-integrating film records the static Bragg signal from the crystal as well as the dynamic Bragg angle as the shock compresses the crystal lattice. Using thin crystals, the transmitted Laue signal from an orthogonal lattice plane may be recorded, both static and dynamic. The Bragg angle changes as the lattice compresses based on a differential of Bragg s Law,

Equation: $\Delta d/d = -\text{Co}\theta\,\Delta\theta$

When the lattice spacing, d, changes by ˜d, the Bragg angle changes by $\Delta\theta$, thus by measuring the change in θ, the change in the lattice spacing d is known and determines the strain on the crystal along a given lattice plane (Fig 2).

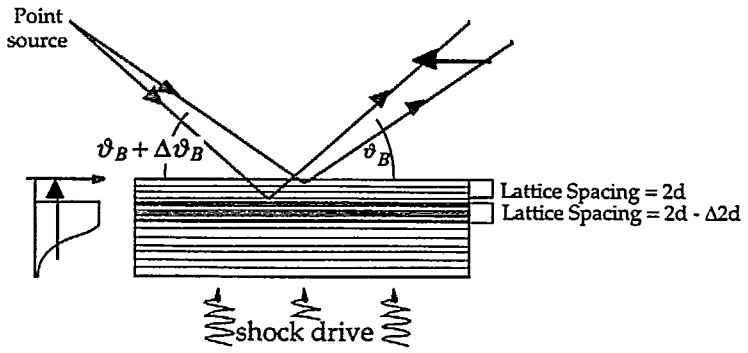

Figure 2: As the shock transits the crystal the unshocked and shocked Bragg angle is generated. An x-ray streak camera can record dynamic change in the Bragg angle as the shock compresses and releases the crystal lattice. (from Wark).

1.2. Experimental set-up and diagnostics

A plastic-coated gold cone confines the K-α x-ray source to a solid angle that includes the Bragg angles (shocked and unshocked) of the silicon (100) (Fig. 3). While one beam of the Los Alamos Trident laser generates a shock in the Si (100) crystal, a second synchronized or delayed beam is focused on the x-ray source material through the larger entrance of the truncated gold cone (Fig. 4). The generated K-shell x-rays exit the truncated apex of the cone and diffract from the unshocked (static) crystal, as the shock reaches the surface, the shocked (dynamic) Bragg signal is recorded (Fig. 5). Experiments have confirmed quantum mechanical code calculations that predict shock wave splitting in silicon.[6] Free-surface velocity measurements of shocked silicon have been incorporated with transient x-ray diffraction. Both a line-VISAR and a point-VISAR have been used to simultaneously measure free surface velocity to correlate with the uniaxial shock compression in silicon. [6-7] Using the known silicon EOS and free surface velocity, the shock pressure in the silicon can be determined.

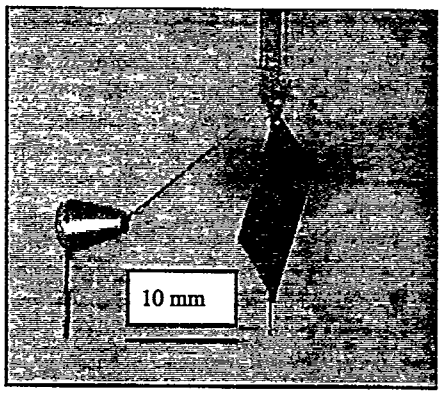

Figure 3: A silicon <100> target (10 mm x 10 mm x 20 m thick) with the x-ray backlighter source mounted so the solid angle of the x-rays include the Bragg angles (static and dynamic). The x-ray source is located inside the gold/plastic cone.

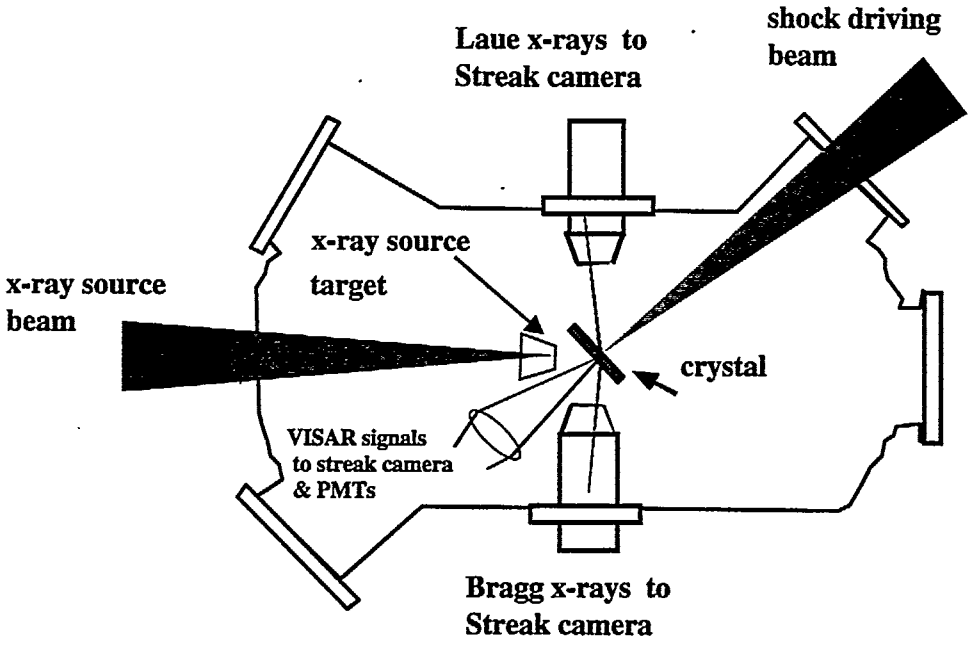

Figure 4: The experimental method used to shock single crystals and determine the static and dynamic Bragg and Laue diffraction angles incorporates two laser beams and two x-ray streak cameras.

1.3. experimental results for silicon and beryllium

1.3.1. Silicon

Several sets of experiments were performed on single crystals of silicon, cut so that the sample surfaces were parallel to the 001 planes of the crystal lattice. Transient x-ray diffraction was used to follow changes to the 004 Bragg reflection and the <400> Laue reflection. Later experiments used the line-imaging VISAR to record the velocity history over a region of the free surface. Experiments were performed with both diagnostics.

As the laser energy increased, the Bragg reflection from the shocked material was observed to deviate by an increasing amount from the unshocked position. The velocity of the sample surface after the arrival of the shock wave was also

observed to increase with laser energy. Above a threshold energy, the shocked Bragg signal split into two closely-spaced lines a short time after it first appeared, and there was evidence of other lines on release. Above the same energy, the shock wave arriving at the surface also split into two waves. The Laue reflection was not observed to change at all under compression, and recovered samples showed no evidence of plastic flow. [7]

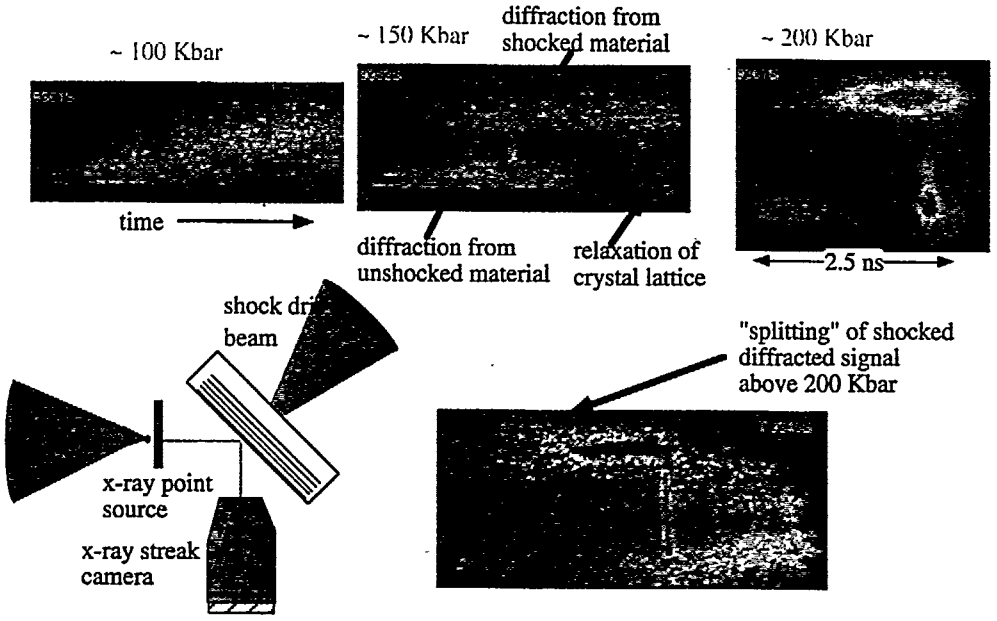

Figure 5: Four different x-ray diffraction streak records at 100, 150, 200 and >200 kbar with time on the horizontal axis (2.5 — 4 ns, full scale) and vertical as increasing Bragg angle representing ~3 — 10 % compression of the lattice. The >200bar showing of the shock splitting.

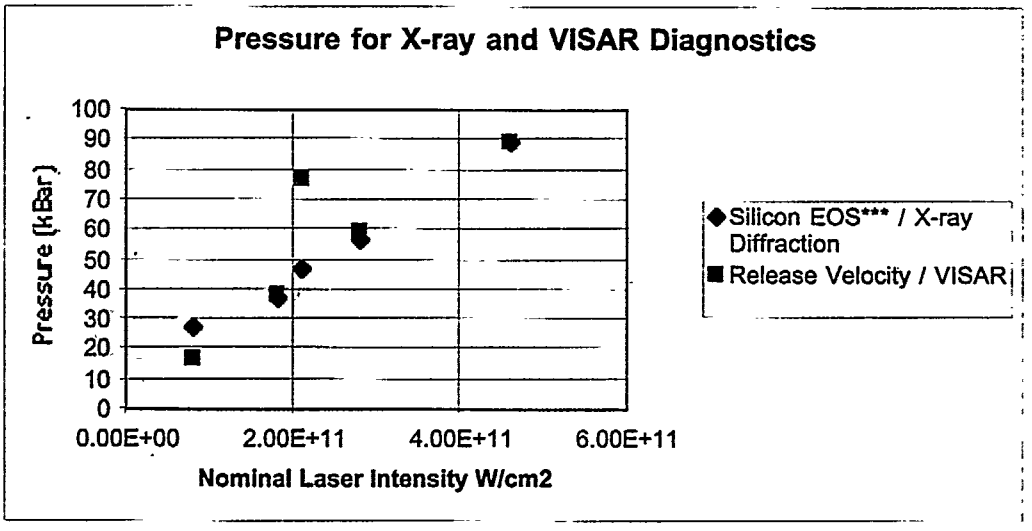

Fitgure 7: Comparison of shock pressure as measured by two independent methods: VISAR free-surface velocity and Bragg angle of compression of the lattice. VISAR with Silicon EOS compared with Bragg lattice compression used to construct a EOS.

The data were interpreted using *ab initio* quantum mechanics to predict the polymorphic equation of state and stresses in uniaxial compression. Taking the compression from the change in the Bragg angle, the free surface velocity predicted using the theoretical equation of state was consistent with the measured free surface velocity (Fig.6). The theoretical equation of state predicted the formation of a double shock structure caused by the phase transition from diamond to body-centered tetragonal. The preliminary quantum mechanical studies of uniaxial compression suggest that shear stresses could be suppressed, explaining the lack of change to the Laue reflection and the lack of plastic flow in the recovered samples. A more detailed analysis of the splitting of the Bragg line and the free surface velocities is in progress; the interpretation requires considerable care because the second shock reaching the free surface has already interacted with the reflection of the first shock. Using the known silicon EOS and free surface velocity, the shock pressure in the silicon can be determined.

1.3.2. Beryllium

We have recently performed a set of experiments on single crystals of beryllium, cut so that the sample surfaces were nominally parallel with the 001 planes. Compared with the silicon crystals, the beryllium samples were more of a mosaic of crystallites separated by low-angle grain boundaries, so the rocking curve of a sample was typically ~2^0, compared with a small fraction of a degree for silicon. In addition, the angular accuracy of cutting the samples was ~1^0, i.e. the mean 001 plane differed by this much from the plane of the surface.

Four samples of beryllium were used for the experiments, and the first was used twice: once with x-ray generation but no shock wave to compare the static signal with the rocking curve, then recovering the crystal and re-using it with a shock wave. The width and shape of the Bragg reflection agreed closely with the rocking curve, indicating that this was the only significant contribution to the width of the diffraction line. In the subsequent four experiments, the laser intensity used to generate the shock wave was increased each time.

Transient x-ray diffraction records, both time-resolved and time-integrated, were obtained from every shot, along with line VISAR records (Fig.7). Detailed analysis is still in progress, but the Bragg records show distinct signals from the unshocked and shocked material. At pressures below ~30 GPa, a single peak appeared in the shocked material, and the deviation in the Bragg angle increased with pressure. At higher pressures, an additional weaker peak appeared at a higher angle, and this angle also increased with pressure (Fig 8.). The unshocked Laue reflection was out of the field of view of the x-ray cameras, but two peaks appeared in the Laue camera on the shots where the additional Bragg peak appeared. One of the Laue peaks moved significantly as the pressure was increased. At lower pressures, the VISAR records showed a two-wave structure where the first wave resulted in roughly the same free surface velocity and the velocity behind the second wave increased with laser intensity. At ~35 GPa, a two wave structure was again seen, except with a higher initial velocity and a significantly longer rise-time for the second wave. At the highest pressure (~48 GPa), a single wave appeared, and had a long rise-time.

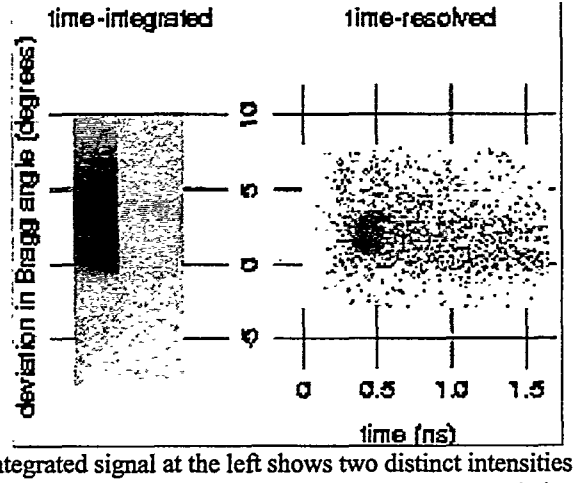

Figure 8: The static Bragg time-integrated signal at the left shows two distinct intensities representing the zero deviation from the static Bragg and a second intensity related to the shocked lattice Bragg angle increase of approximately 3 degrees. The x-ray time-resolved is located in the right side of the image.

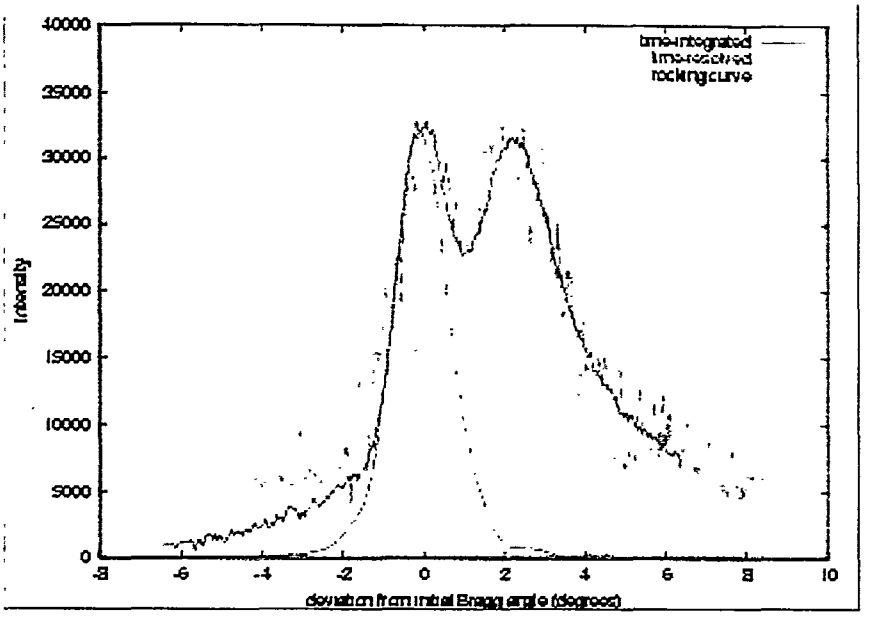

Figure 9: The narrow Gaussian shaped signal represents the measured rocking curve for a Beryllium crystal, The smooth bimodal signal is the time-integrated signal along with the x-ray streak camera (time resolved) collapsed signal. Alignment of signals confirms any significant change is the Bragg angle is a result of lattice compression and not another phenomona.

An initial interpretation of these results was made with the aid of an *ab initio* quantum mechanical equation of state for beryllium, including the hexagonal and body-centered cubic phases. The transition pressure on the shock Hugoniot was predicted to be ~35 to 40 GPa. We suggest that below ~35 GPa, the Bragg records show a single shocked state in the hexagonal structure. The VISAR records appears to show an elastic precursor followed by a plastic wave. Above ~35 GPa, it seems likely that beryllium starts to transform to the body-centered cubic structure, creating an additional reflection in the Bragg record and the first lines in the Laue record. Around 35 GPa, the VISAR record probably showed a plastic shock in the hexagonal structure (with no elastic precursor), followed by a broader structure corresponding to the phase change to body-centered cubic. Above ~45 GPa, the VISAR record then showed a single shock combined with the phase change into body-centered cubic. This explanation seems to be consistent with the data and the theoretical equation of state, but we emphasize that it is based on the preliminary analysis only.

2. Laser-launched flyer plates

2.1. experimental method for laser plate launch

Flyer plate launch techniques that were initially used with commercial lasers but recently have been applied to the Trident laser. Trident is operated at the fundamental mode, 1.054 m, with long pulse length >60-ns FWHM with various controlled temporal and spatial profiles. LASNEX code calculations have been used to model the laser interaction with materials.[9] A multi-layer coating of carbon/metal/metal oxide is vacuum deposited on a transparent substrate.[10] When a laser beam is pulsed through the substrate, the energy is absorbed within a few skin depths (~150 nanometers) and converted to a plasma.[11-15] The confined high- pressure plasma between the much thicker substrate and the thinner multi-layer coating accelerates the remaining coating away from the substrate. The remaining coating layer and the attached material functions as the flyer plate (Fig. 9). Plate thickness 2 —100 m has been used, but plates >500 μm thick should be possible. Depending on flyer plate impedance, thickness, and laser pulse duration and energy fluence, terminal velocities of 0.1 - > 6 km/sec (μm/ns) can be obtained within 10 — 200 ns. A 1-D plate can be launched with a near-spatially flat top laser beam of 1 — 3 GW/cm^2 and a temporal profile to accommodate the plate thickness and impedance. Ideal laser-launched plates perform the same as larger plates from gas guns, i.e. accelerate the plate uniformly and minimize ringing in the plate on acceleration to mitigate internal spall and shock heating, highest possible velocity while maintaining, and largest practical diameter-to-thickness ratio. Laser-launched flyer plates complement gas gun experiments for material shock hydrodynamics.

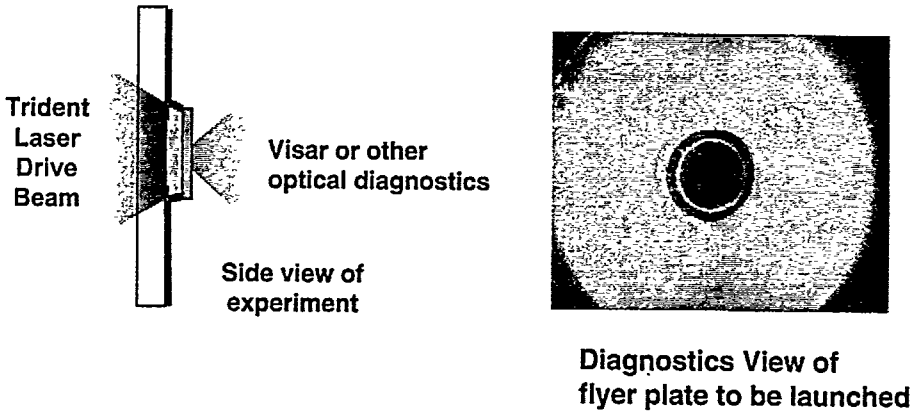

Figure 9: The laser is pulsed through the sapphire substrate and the energy is deposited in the first layer of material creating a plasma. The trapped plasma expands accelerating the material away from the substrate .

1.2. *experimental results for plate launch*

The laser-launched flyer plates velocity profiles are recorded using a line-imaging VISAR across the diameter of the flyer plate and recorded with an electronic streak camera. The flyer plate is attached to an ablative layer. The diameter of the plate is illuminated with a 660-nm 60-ns FWHM laser. The reflected light is directed into the VISAR with vertical fringes imaged on the output beam splitter and re-imaged on the horizontal slit of the streak camera. The line-imaging VISAR confirms the one-dimensionality, acceleration and terminal velocity. With most experiments the temporal resolution is < 100-ps and spatial resolution approximately 30- m (Fig 10).

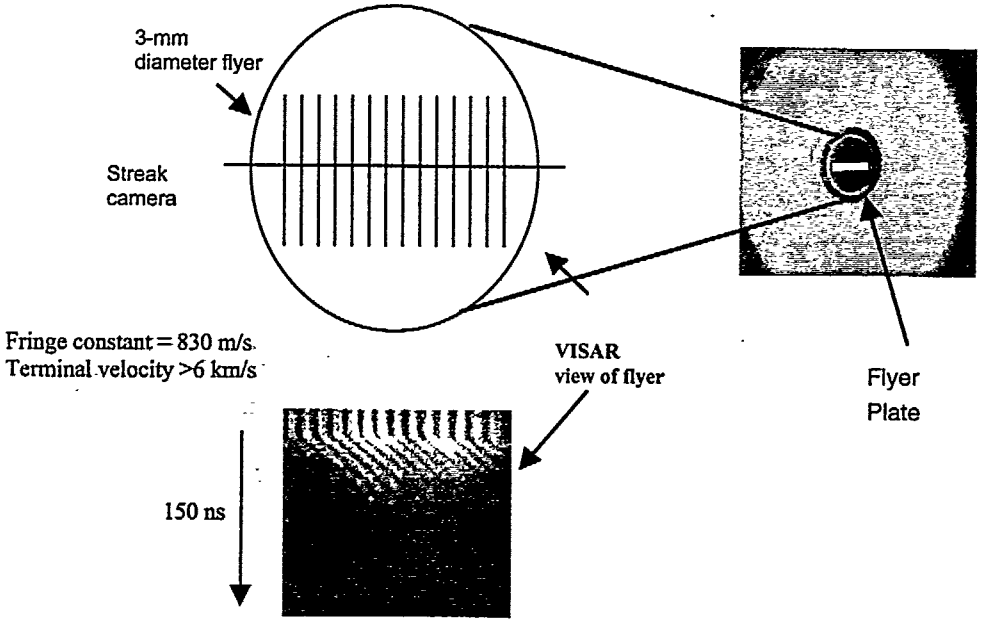

Figure 10: An experimental view of the flyer plate, a line-VISAR image of the flyer plate, and a streak camera record of the line-VISAR data. The fringes moving to the right represent a flyer plate acceleration with a terminal velocity greater than 6 km/s. The fact the fringe are evenly spaced indicated the one-dimensional plate launch.

Plates are ideally accelerated without imparting a significant shock to avoid shock heating, plate ringing and internal spall stress in the plate. Confined metals such as aluminum require a power density of ~ 1 GW/cm^2 before the plasma is formed and can reflect back up to 20% of the energy before , depending on pulse shape. In addition to laser pulse shaping, coupling efficiency can be improved by using a lighter element as the driving plasma. Previously thin (3-10 m) flyer plate experiments and now thick (‡50 m) indicate improved energy coupling and desired acceleration of plates (Fig 11).

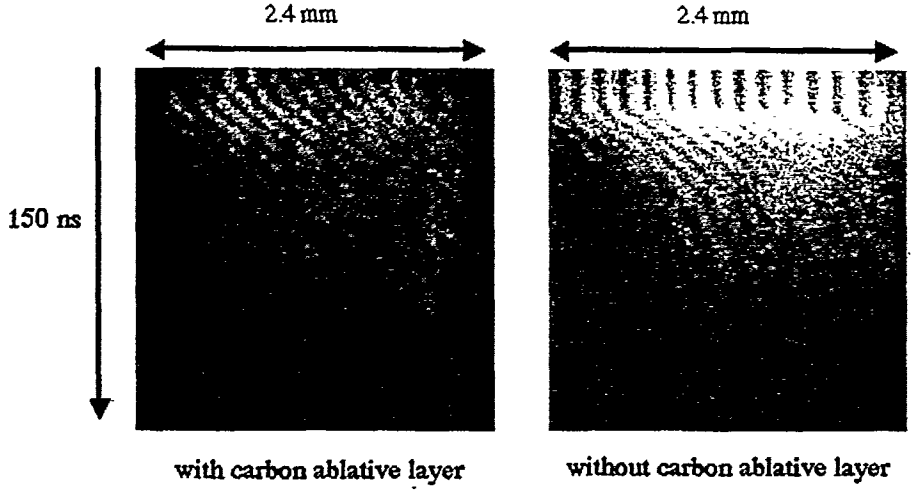

Figure 11: Flyer plate acceleration (fringe motion, lt. to rt.) is recorded with electronic streak cameras coupled to 2K x 2K CCD. Each fringe shift represents a change in velocity of 830 m/s. Both flyer plates were launched with laser pulse lengths that were approximately 50X the round trip shock velocity in the plates. The flyer plate on the left included a carbon ablative layer at the transparent interface. As can be seen in the record, the plate acceleration does not have the abrupt acceleration of the flyer on the right image. The carbon ablative layer results in approximately 10 % higher velocity.

6.Conclusions

Large laboratory lasers coupled with optical and x-ray high-speed diagnostics, and interferometry have been used to study dynamic response of single and polcrystalline materials to shock compression and release from 0.1 - >200 GPa. Elastic, elastic-plastic response and phase change has been determined. One-dimensional laser-launched plates have been accelerated and monitored for velocity, acceleration and planarity using line-imaging VISAR.

7. Acknowledgements

We thank the following Los Alamos individuals who assisted with this work. D. Thoma and J. Cooley for providing the single crystal beryllium, and R. Springer for measuring the static rocking curves for the crystals. R. Perea fabricated the test assemblies. T. Sedillo and the Trident crew provided the diagnostic support and laser operations. Allan Hauer has advised, consulted, encouraged and supported us with this endeavor.

8. References

1. A. A. Hauer, J. S. Wark, *et al*, Proceedings of the SPIE - The International Society for Optical Engineering, Vol. 3157, (Applications of X Rays Generated from Lasers and Other Bright Sources, San Diego, CA, USA, 31 July-1 Aug. 1997.) SPIE-Int. Soc. Opt. Eng, 1997. p.72-83.
2. J. S. Wark, *et al*, Phys. Rev. B **40**, 5705 (1989).
3. N. Woolsey and J. Wark, J. Appl. Phys. **81**, 3023 (1997).
4. P. Rigg and Y. Gupta, Appl. Phys. Lett. **73**, 1655 (1998).

5. A. A. Hauer, G. A. Kyrala, Time-resolved Diffraction, eds. J. R. Helliwell and P. M. Rentzepis, Oxford Science Publications, 1997
6. Andrew Forsman, to be published
7. P. M. Celliers , G .W. Collins, L. B. da Silva D. M. Gold, R. Cauble, Applied Physics Letters Vol. 73,p 1320, 1998
8. Damian Swift, to be published
9. D. L. Paisley, R. H. Warnes, and R. A. Kopp, Laser-driven flat plate impacts to 100 Gpa with sub-nanosecond pulse duration and resolution of material property studies, Shock Compression of Condensed Matter-1991, S. C. Schmidt, et al., eds., Elsevier Science Pub. B. V., pp. 825-828.
10. US Patent 5,301,612, Carbon-assisted flyer plates, D. L. Paisley, D. B. Stahl, Los Alamos
11. US Patent 5,046,423, Laser-driven flyer plate, D. L. Paisley, Los Alamos
12. US Patent 5,029,528, Fiber optic mounted laser driven flyer plates, D. L. Paisley, Los Alamos
13. D. L. Paisley, Laser-driven miniature flyer plates for one-dimensional impacts at 0.5 — 6 km/s, Shock-Wave and High-Strain Rate Phenomena in Materials, EXPLOMET, eds. M. C. Meyers, et al., eds, Marcel Dekker Inc. 1992.
14. S. Watson, J. E. Field, Measurement of the ablated thickness of films in the launch of laser-driven flyer plates, J. Physics D: Applied Physics, 33(2000) pp.170-174
15. K. Ito, T. Aizawa, D. L. Paisley, Laser-Driven Shock Device for Real-Time Hugoniout Measurement, Rev. High Pressure Science and Technology, Vol. 7 (1998), p 876-878